Polymer 49 (2008) 3629–3638

Contents lists available at ScienceDirect

Polymer

journal homepage: www.elsevier.com/locate/polymer

High-resolution ^{19}F and ^{1}H NMR of a vinylidenefluoride telomer

Philip Wormald [a,*], Bruno Ameduri [b], Robin K. Harris [c], Paul Hazendonk [d]

[a] School of Chemistry, University of St Andrews, Purdie Building, St Andrews KY16 9ST, UK
[b] Ingénierie et Architectures Macromoléculaires, Institut Charles Gerhardt – UMR(CNRS) 5253, Ecole Nat Sup de Chimie de Montpellier, 8 Rue de l'Ecole Normale, F-34296 Montpellier Cedex, France
[c] Department of Chemistry, University Science Laboratories, South Road, Durham, DH1 3LE, UK
[d] Department of Chemistry and Biochemistry, 4401 University Drive, University of Lethbridge, Alberta, T1K 3M4 Canada

ARTICLE INFO

Article history:
Received 24 April 2008
Received in revised form 20 June 2008
Accepted 26 June 2008
Available online 2 July 2008

Keywords:
^{19}F and ^{1}H NMR
Correlation spectroscopy
Vinylidenedifluoride

ABSTRACT

The reaction products of vinylidenefluoride (VDF) with methanol as a telogen have been analysed in the solution state by ^{1}H and ^{19}F nuclear magnetic resonance (NMR) spectroscopy. High-resolution ^{19}F and ^{1}H NMR spectra were achieved using high-power ^{1}H and ^{19}F decoupling, respectively, giving superior resolution and revealing previously unresolved signals of the vinylidenefluoride telomer (VDFT). ^{1}H and ^{19}F homo- and hetero-nuclear scalar coupling constants are presented and the spectra of functional groups and reverse units (including the identification of short-chain structures) are discussed. Furthermore, the application of ^{19}F or ^{1}H decoupling for the correct assessment of reverse-unit content and degree of polymerisation is demonstrated. This work highlights the need for high-resolution NMR spectroscopy to determine both the chemical structure and the composition of these important fluoropolymers.

1. Introduction

The large chemical shift dispersion of fluorine nuclear magnetic resonance (NMR) led to some of the first spectra determining the composition and structure of synthetic fluoropolymers [1–3]. These first structures were deduced from ^{19}F NMR spectra without ^{1}H decoupling, revealing the characteristic head-to-head (H–H) and head-to-tail (H–T) monomer sequences of poly(vinylidene fluoride) (PVDF), which are now well known in the literature. The development of high-field magnets combined with the acquisition of ^{1}H and ^{19}F with ^{19}F and ^{1}H decoupling, respectively, offers a great improvement in spectral resolution. However, many laboratories do not have this facility, partially due to cost, and many assignments are still made using spectra of lower resolution. The problems of resolution and subsequent signal assignment for fluorinated polymers are often further complicated because analyses are made on samples of raw synthetic samples, which contain a mixture of reaction products (i.e. with varying chain lengths and functional groups) requiring estimations of reverse units and end-chain groups. Such analyses are also important for the understanding of the polymerisation reactions and thus for finding improved efficiencies for producing fluoropolymers. Separation procedures have substantial drawbacks and NMR is the only technique sufficiently powerful to determine structural details of the reaction products *in situ*.

Multinuclear correlation experiments have been implemented on samples related to PVDF, usually to gain resolution for a specific group of signals [4–6]. The assignments are often deduced from spectra of model compounds or of samples obtained by various synthetic pathways [7–9], in the case of VDF telomers obtained from methanol. ^{1}H and ^{19}F solution-state NMR spectroscopy has revealed the presence of $-CH_3$, $-CH_2OH$ and $-CF_2H$ end groups, [10–12] but poor resolution often inhibits the identification of signals which associate them with the adjacent main-chain or other structures. Furthermore, without decoupling the overlap of signals is considerable due to the extent and magnitude of ^{1}H and ^{19}F homo- and hetero-nuclear scalar couplings [13]. We are here concerned with relatively small PVDF samples, i.e. with vinylidene fluoride telomer (VDFT) products. However, no extensive investigation using one- and two-dimensional solution-state NMR experiments on such samples by observation of ^{1}H and ^{19}F resonances while decoupling ^{19}F and ^{1}H, respectively, appears to have been carried out previously.

Comparison of coupled and decoupled spectra enables the scalar coupling constants to be determined, leading to a more accurate structural evaluation. Typical (H,F) coupling constants found in the literature for PVDF main-chain CF_2CH_2 groups are $^{3}J_{F,H} \sim 16$ Hz, and $^{4}J_{H,H} = 0$–5 Hz, while $^{4}J_{F,F}$ is typically 10 Hz. [14–16] The reverse unit $-CF_2CF_2CH_2CH_2-$ provides a well-documented feature in the spectra of VDF materials, yet splittings

* Corresponding author. Tel.: +44 (0) 1334 463382; fax: +44 (0) 1334 463808.
E-mail address: pw22@st-andrews.ac.uk (P. Wormald).

0032-3861/$ – see front matter © 2008 Elsevier Ltd. All rights reserved.
doi:10.1016/j.polymer.2008.06.043

arising from $^{3}J_{F,F}$ (0–5 Hz) and $^{3}J_{H,H}$ (3–12 Hz) are often not resolved and therefore only a limited number of values have been documented for such systems. Usually the $^{3}J_{F,H}$ coupling constants involved in reverse units are also reported to be of the order of 16 Hz [17]. Further couplings of importance are those of the end-groups showing $^{2}J_{F,H}$ (54.5 Hz) and $^{3}J_{H,H}$ (4.4 Hz) for H–CF_2–CH_2–, $^{3}J_{H,H}$ (7.5 Hz) for CH_3–CH_2–, and $^{3}J_{F,H}$ (19.3 Hz) for CH_3–CF_2– [16]. For the observation of small coupling constants, the linewidth and resolution of the spectrum are obviously of great importance, which is probably the main reason why $^{3}J_{F,F}$ and $^{4}J_{H,H}$ coupling effects are seldom seen in spectra of high molecular weight PVDF polymers. The $^{n}J_{F,F}$ couplings do not follow the same general behaviour as $^{n}J_{H,H}$ couplings. It is possible for groups in straight-chain fluorinated compounds such as VDF to have vicinal $^{3}J_{F,F}$ couplings near to zero, whereas $^{4}J_{F,F}$ coupling constants can be quite large, ~10 Hz. This must be taken into consideration when assigning coupling constants and thereby determining the structure. ^{19}F COSY spectra can often give more correlations than are typically found in a ^{1}H-COSY spectrum. Whilst many examples of ^{1}H/^{19}F heteronuclear correlation experiments have been published [18,19], few have been applied to polymeric fluorine systems and it is noted that ^{19}F/^{19}F TOCSY experiments involve a difficulty in creating a spin-lock over the entire ^{19}F chemical shift range [20]. A ^{19}F-COSY spectrum has revealed unambiguously the pentad assignments in isoregic poly(vinyl fluoride) [21] and on aregic poly(vinylidene fluoride) [22,23], such that the main regiosequence assignments out to the heptad level were verified. One major advantage of the 2D COSY experiment is that correlations are observable when couplings between multiplet systems are not resolved in 1D spectra. This is usually the case for polymers, where couplings as large as 7–10 Hz may not be resolved because of the 10 Hz linewidths. In our earlier work on PVDF [24] we showed that a 2D COSY spectrum revealed peaks at approximately −107 ppm, which were assigned to possible CF sites at chain-branching positions, as these signals showed no off-diagonal cross peaks. The literature suggests assignments for some of these peaks to –CF_2–CH_3 end groups and offers chemical shift calculations to justify assignments of other peaks in this region to chain branching [25,26]. Any variations such as hydroxyl groups, defect units or modification of existing functionalities are of great importance, specifically for further chemical modification resulting in enhanced material properties for applications in, for example, modified membranes in polymer electrolyte fuel cells [27,28]. In earlier work [24] we suggested an extended structure for the reverse units and CF_2 groups adjacent to them. However, the corresponding protons of the reverse units and end chains and any correlations of protons to the fluorine signals at approximately

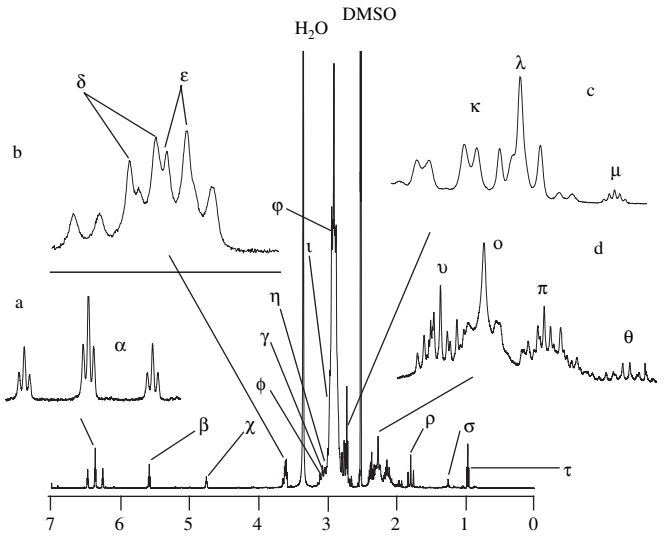

Fig. 1. The 500 MHz ^{1}H spectrum of VDFT in DMSO-d_6 at 22 °C without ^{19}F decoupling, together with expansions a–d. Greek lettering gives the proton assignments seen in Table 1.

Table 1
Proton chemical shift and coupling data for VDFT[a] together with assignments for the proton resonances

δ (^{1}H) ppm	Relative intensity[b]	Multiplicities[c]		Notation	Coupling constants[d]		Functionality[e]
		Coupled	Decoupled		$^{3}J_{H,H}$	$^{3}J_{F,H}$	
6.360	2	tt	t	α	4.5	54.5 (^{2}J)	–CH_2–CF_2H
5.578	0.5	t	t	β	6.5		–CF_2–CH_2–O**H**
4.751	0.5	t	t	χ	6.0		–CH_2–CH_2–O**H**
3.622	1	td	t	δ	6.5	14.5 (^{3}J)	–CF_2–**CH_2**–OH
3.600	1	td	td	ε	6.5 and 4.8		–CH_2–**CH_2**–OH
3.348							H_2O
3.072	2	s	s	ϕ	NR		–CF_2–CF_2–**CH_2**–CF_2–
3.012	0.5	s	s	γ	NR		See the text
2.997	–	s	s	η	NR		See the text
2.963	–	s	s	ι	NR		See the text
2.905	54	s	s	φ	7.3	16.0 (^{3}J)	–CH_2–CF_2–**CH_2**–CF_2–CH_2–
2.837	0.5		s	ϖ	NR		See the text
2.792	0.5		s	ω	NR		X–**CH_2**–CF_2–CH_2–CH_3
2.753	4	qd	d	κ	4.4	16.5 (^{3}J)	–CF_2–**CH_2**–CF_2H
2.720	2	t	t	λ	7.5		–CF_2–CH_2–**CH_2**–X
2.653	0.2	q	q	μ	NR		$(CH_3)_3$–CO–**CH_3**
2.358	2	tt	t	ν	6.5	16.5 (^{3}J)	–CF_2–**CH_2**–CH_2–X
2.267	4	t	s	o	NR	16.5 (^{3}J)	–CF_2–**CH_2**–CH_2–CF_2–CF_2–CH_2–
2.138	2	tt	t	π	6.5	16.5 (^{3}J)	–CF_2–**CH_2**–CH_2–OH
1.961	0.5	tqu	q	θ	6.5	16.5 (^{3}J)	–CF_2–**CH_2**–CH_3
1.794	1	t	s	ρ		19.5 (^{3}J)	–CF_2–CF_2–**CH_3**
1.252	0.2	s	s	σ			$(CH_3)_3$CO–**CH_3**
0.967	0.5	t	t	τ	7.5	20.0 (^{3}J)	–CF_2–CH_2–**CH_3**

NR = Not resolved and no intensity measurable due to overlapping signal unless otherwise stated.
[a] The numerical data are taken from the fluorine-decoupled proton NMR spectrum, except for the values of J_{F-H}, which come from the fluorine-coupled proton spectrum.
[b] Values in brackets are for the minor components and multiplied by 4.
[c] d = doublet, t = triplet, qu = quartet, q = quintet.
[d] Coupling constants are given to the nearest 0.5 Hz.
[e] The relevant hydrogen atom is in bold typeface.

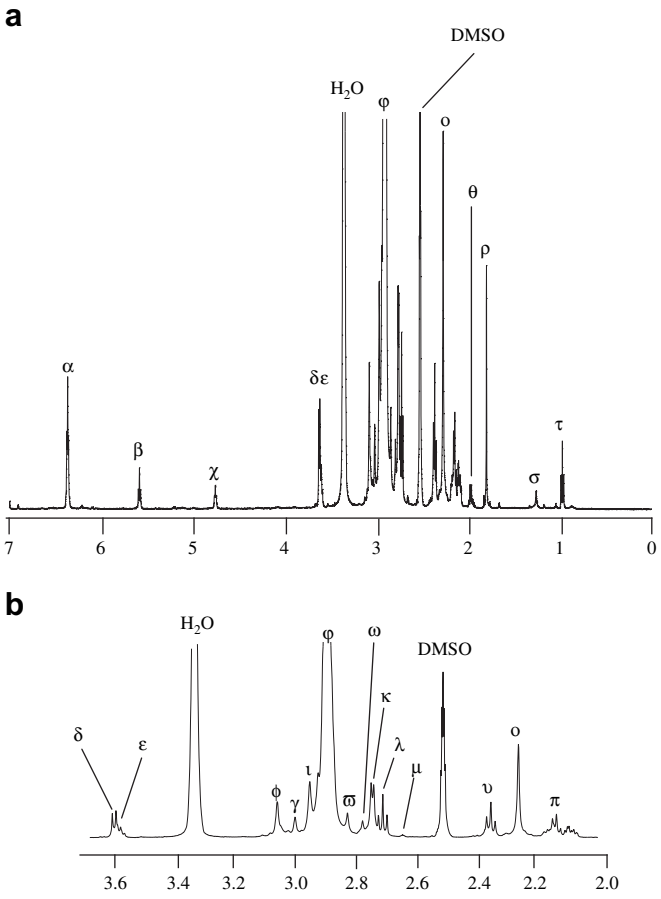

Fig. 2. The ^{1}H spectrum of VDFT in DMSO-d_6 at 22 °C with ^{19}F decoupling (a) and an expansion (b). All assignments are given in Table 1.

−106 and −108 ppm were not investigated. Recently, we studied the reaction products of VDFT by solid-state NMR [29] which revealed a great difference in the solid characteristics and macroscopic properties of VDFT compared to those found by our previous solid-state NMR studies on PVDF [24,29–32]. Therefore, in this paper, we characterize VDFT by ^{19}F and ^{1}H solution-state NMR spectroscopy to evaluate, structure, defect-unit content, degree of polymerisation and the effect decoupling has on the analysis. Coupling constants are reported where possible, but this is greatly dependent upon linewidth and scalar coupling attenuation (*vide supra*) for $^{3}J_{F,H}$ $^{3}J_{F,F}$ and $^{4}J_{F,F}$, including relevant $^{1}J_{H,H}$ couplings [13]. Furthermore, assignments of minor peaks in the ^{1}H and ^{19}F spectra, including chain end-groups and short-chain VDFT fragments are offered. Any new information provided by these assignments could influence perceived synthetic reaction pathways as the proton and fluorine spectra are often employed to deduce reaction products and their intermediates [10]. Geminal (F,F) coupling constants are large (ca. 200 Hz) and in principle can affect spectra. In most cases, the two fluorines of a CF_2 group and the two protons of a CH_2 group are chemically (but not magnetically) equivalent, and further considerations are required [24]. Thus, the nuclei of a main-chain CF_2–CH_2 group will give an $[AX]_2$ contribution to the total spin system. However, the magnitude of $^{2}J_{FF}$ will render the result indistinguishable from that of an A_2X_2 system [33]. When the CF_2 fluorines are chemically non-equivalent, which only occurs when the group is adjacent to a chiral centre (e.g. at branching points), the situation could be more complicated, but even here such fluorines are, in practice, rendered effectively equivalent by the coupling. Of course, the full spin system of a VDFT is actually very complex. In this work we analyse the radical telomerisation of VDF in methanol initiated by di-*tert*-butyl peroxide (DTBP) as previously discussed [10].

2. Experimental

The VDF telomer was prepared as described in the literature [10]. The solution-state spectra were recorded at 22 °C on a Bruker 500 MHz Avance spectrometer equipped with a QNP probe and operating at 499.78 MHz for ^{1}H and 470.21 MHz for ^{19}F. The solvent was dimethylsulfoxide-d_6 (DMSO-d_6). ^{19}F chemical shifts were measured and are quoted relative to the signal for a replacement sample of $CFCl_3$ and ^{1}H shifts are relative to the signal for tetramethylsilane. The one-dimensional ^{19}F spectra were recorded with the following parameters: spectral width 28 kHz; data size 32K; pulse delay 1 s; pulse duration (90°) 11.9 μs. The one-dimensional ^{1}H spectra had a 7 kHz spectral width, pulse delay of 1 s and pulse duration (90°) of 10.5 μs. Standard Bruker pulse sequences were

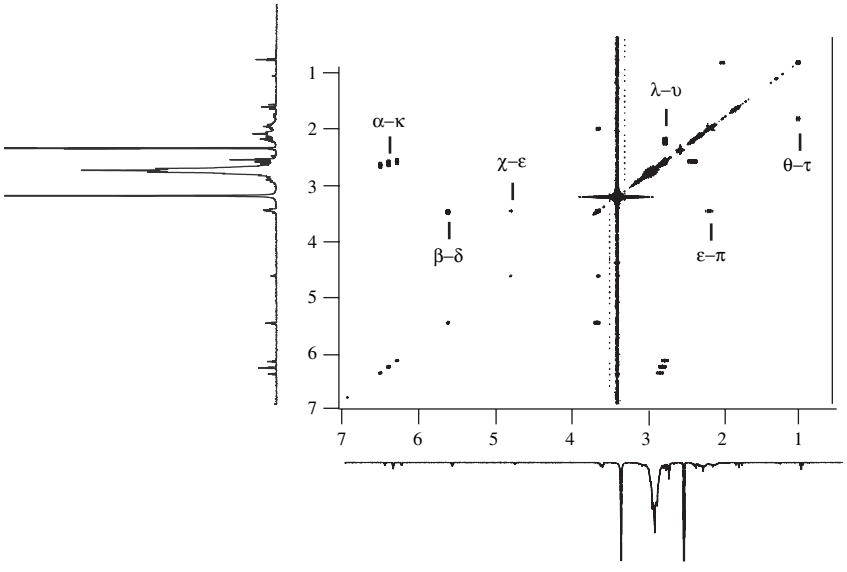

Fig. 3. The ^{1}H COSY of VDFT in DMSO-d_6 at 22 °C without ^{19}F decoupling. The proton assignments are given in Table 1.

Table 2
Proton homonuclear correlations for VDFT

δ (^{1}H)/ppm[a] for correlations		Assignment	Integral ratios
6.360 (tt)–2.753(qd)	α–κ	$-CF_2-CH_2-CF_2H$	1–2
5.578 (t)–3.622(d)	β–δ	$-CF_2-CH_2-OH$	1–2
4.751 (t)–3.600(dt)	χ–ε	$-CH_2-CH_2-OH$	1–2
3.600 (dt)–2.138(tt)	ε–π	$-CF_2-CH_2-CH_2OH$	2–2
2.720 (t)–2.358(t)	λ–ν	$-CH_2-CH_2-CF_2$	1–1
1.961 (tq)–0.967(t)	θ–τ	$-CH_2-CH_2-CF_2$	1–1

[a] d = doublet, t = triplet, qu = quartet, q = quintet.

used for ^{1}H and ^{19}F COSY and ^{1}H/^{19}F HETCOR spectroscopy, with 20 kHz spectral widths along the t_1 and t_2 directions, a 256 × 4K data-point matrix for ^{19}F and a recycle delay of 3 s. For ^{1}H experiments, 4 kHz spectral widths in t_1 and t_2 and a 256 × 2K data point matrix were used in the COSY experiments. Similar parameters were used in the HETCOR experiment.

3. Results and discussion

3.1. Major signals in the ^{1}H and ^{19}F spectra of VDFT

Poly(vinylidenefluoride) (PVDF) is a very interesting industrial polymer, which possesses remarkable properties for high Tech applications. Its melting point and hence its temperature of processing depends on its crystallinity, which is linked to its defects of chaining. These properties are of course of similar interest for the reaction of VDF with di-*tert*-butyl peroxide (DTBP) in methanol, which is shown below, where the structure for the major reaction products has been based on low resolution NMR data [10] with no decoupling applied.

$$HOCH_3 + nH_2CF_2 \xrightarrow{DTBP} HOCH_2-(C_2H_2F_2)_n-H + R-\text{oligo (VDF)}$$

Here, we will discuss the structure of the reaction products using ^{1}H and ^{19}F NMR with decoupling, and correlation spectroscopy,

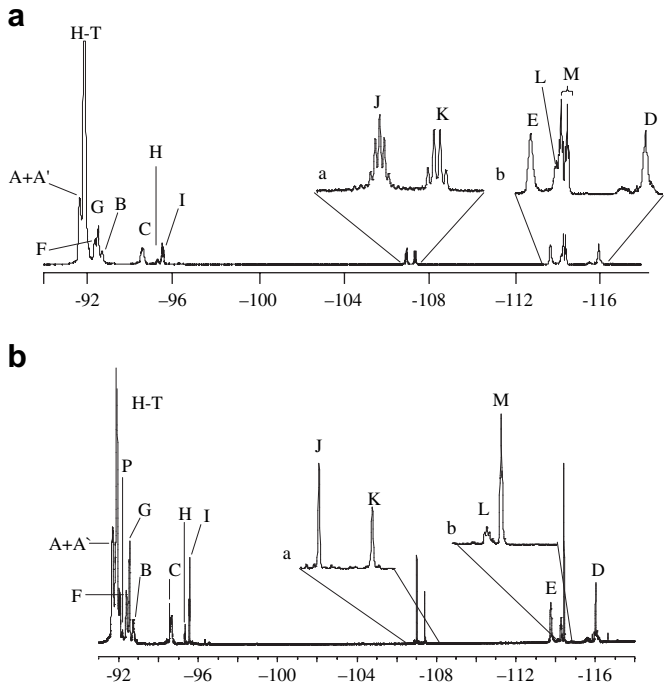

Fig. 4. ^{19}F proton-coupled (a) and proton-decoupled (b) spectra of the VDF telomer in DMSO-d_6 at 22 °C. Both parts show expansions of branching/chain-end signals (insets a) and reverse-unit and chain-end signals (insets b).

Table 3
Fluorine chemical shift and coupling data for VDFT, together with designations of the fluorine resonances

δ (^{19}F) ppm	Relative intensity	Multiplicities		Coupling/Hz		Designation
		Coupled	Decoupled	$^3J_{FH}$	$^3J_{FF}$	
−91.690	4	m	m			A + A′
−91.897	55	m	m			H–T Main Chain
−92.034					9.5	N
−92.078					9.5	O
−92.191	0.5 (2)				9.5	P
−92.390	2	m	m			F
−92.550	4	m	m			G
−92.735	2	m	m			B
−94.577	1 (2)	m	t		9.5	C′
−94.659	2	m	m			C
−95.330	0.5 (2)	m	t		9.5	H
−95.568	2	m	t		9.5	I
−107.010	1 (2)	q	s	14.7		J
−107.415	1 (2)	q	s	19.8		K
−113.768	3	m	m			E
−114.319	1	m	t		10.1	L
−114.423	4	ttd	t	16.5[a]	[b]	M
−116.226	2	m	m		14	D

[a] Also $^2J_{FH} = 54.5$ Hz.
[b] $^4J_{FF} = 6.0$.

reporting coupling constants where possible and showing the necessity of these techniques to derive a more correct structural interpretation, and assess the polymers' physiochemical properties i.e. reverse unit content and the degree of polymerisation.

Firstly, most of the major signals in the ^{19}F and ^{1}H spectra of VDFT (with and without decoupling) and their structural assignment by correlation spectroscopy will be discussed, since many of these signals are common to VDF-type structures and are well known [10,16,22]. Fig. 1 shows the fluorine-coupled proton spectrum of VDFT with expansions (a, b, c and d). This spectrum involves both $^3J_{H,H}$ and $^3J_{F,H}$ coupling patterns, as listed in Table 1 together with assignments, integrals and magnitudes of $J_{F,H}$ couplings. The peaks are denoted by Greek letters and the assignments become clear when the splitting patterns are considered, and the results of two-dimensional experiments are evaluated. The fluorine-decoupled proton spectrum (Fig. 2) shows an increase in proton resolution, which allows a more accurate determination of chemical shifts and proton homonuclear coupling strengths (as given in Table 1 and quoted in the text below), together with identification of the heteronuclear $^3J_{F,H}$ coupling constants by comparison with the fluorine-coupled proton spectra. The relative signal intensities, given in Table 1, were obtained by integration of the fluorine-decoupled spectrum only. The ^{1}H COSY (Fig. 3 and Table 2) shows the proton-to-proton coupling, with signal assignments given in Table 1. Fig. 4a and b shows the ^{19}F spectra (proton-coupled and proton-decoupled, respectively).

The one-dimensional spectra contain a number of signals that are well known in the literature. An intense quintet at 2.905 ppm (φ) (Fig. 1) is identified as the main-chain protons in $-CF_2-CH_2-CF_2-$ structures of the polymer backbone [10–12]. This signal is reduced to a broad singlet in the ^{19}F-decoupled spectra (Fig. 2), with no visible splitting. The corresponding fluorine signal of the main chain is seen at −91.897 ppm (H–T) in Fig. 4 (see also Table 3). These signals show very similar relative integral values in the proton and fluorine spectra, respectively. The decoupling reveals new low-intensity signals in the main-chain region for both spectra, as will be discussed later.

The proton resonance at 6.360 ppm (α) for $-CH_2-CF_2H$ shows a characteristic triplet of triplets pattern (Fig. 1), with $^2J_{H,F}$ (54.5 Hz) and $^3J_{H,H}$ (4.5 Hz) coupling constants typical of such end chains [16]. The signals α and κ couple, as seen in the ^{1}H COSY (Fig. 3 and

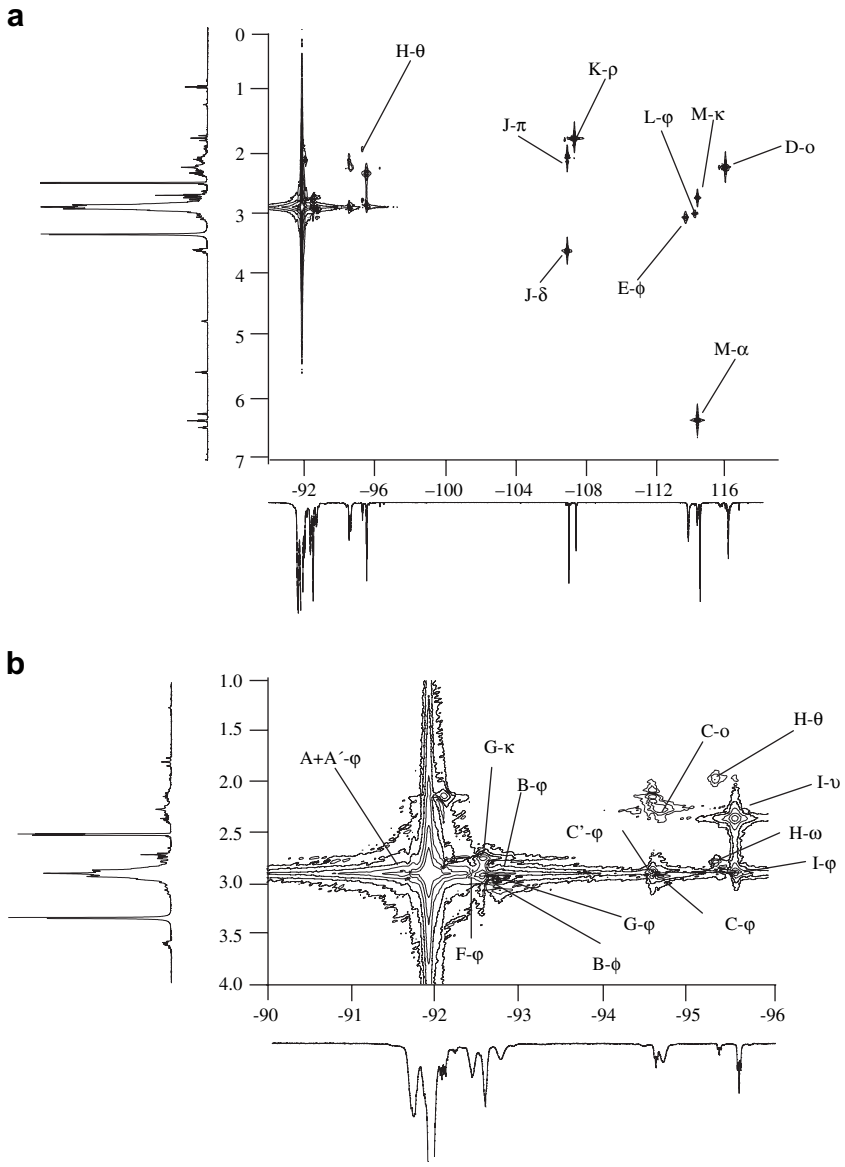

Fig. 5. ^{1}H–^{19}F HETCOR spectrum of the VDF telomer in DMSO-d_6 at 22 °C (a) and expansion of the region around the main-chain signals (b).

Table 2). The signal κ is a quintet of doublets (Fig. 1c), which becomes a doublet when fluorine-decoupled (Fig. 2) and therefore has two CF_2 groups adjacent to it, coupled by $^{3}J_{F,H} \sim 16$ Hz, and one CH group. The signal M seen in the fluorine spectrum (Fig. 4a, inset b) is assigned to the fluorine in the $–CH_2–CF_2H$ end-group [10,11,16]. This signal shows ^{19}F, ^{1}H coupling, causing a doublet splitting with $^{2}J_{F,H} \sim 54.5$ Hz, and is split further into a triplet of triplets ($^{3}J_{F,H}$ of 16.5 Hz and $^{4}J_{F,F}$ of 6.0 Hz). The $^{19}F/^{1}H$ HETCOR spectrum (Fig. 5 and Table 4) verifies the proton assignments of signals α and κ to end-chain $CH_2–CF_2H$ by demonstrating correlations to fluorine group M and (for κ) to fluorine group G. Furthermore, the ^{19}F COSY (Fig. 6) shows that groups giving the signals M and G are near neighbours, proving that the end-group structure is φ–G–κ–M–α (Scheme 1).

A complex triplet (o) in Fig. 1 at 2.267 ppm is in the region anticipated for the methylene groups of the reverse unit $–CH_2–CH_2–CF_2–CF_2–$ [23]. The ^{19}F-decoupled spectrum of the same resonance (Fig. 2) gives only a singlet, i.e. showing no (H, H) splitting. One would expect to see a second-order $[AB]_2$ pattern for these protons in the fluorine-decoupled spectrum, with additional splittings in the fluorine-coupled spectrum. The linewidth of the decoupled signal is ~6 Hz. We assume the resonance arises from both methylene groups of the reverse units, the protons having almost identical chemical shifts so that the signals merge to form a singlet. A full assignment of the defect unit signals and those of the adjacent fluorine groups has been given [24] but is also described in this paper under Section 3.

The less intense signals in the spectra present a greater challenge for interpretation. Many of these signals have been previously assigned by more tentative methods.

3.2. The occurrence of branching and/or end groups

It has been suggested that the fluorine signals in the region between −106 and −108 ppm in the ^{19}F spectrum of VDF materials (Fig. 4a and b) derive from branching of the main chain [23,24] though no NMR spectra have convincingly confirmed all the signals in this region. We now attempt to clarify the nature of these signals and refer to the proton spectrum in Fig. 1, which shows a triplet at 5.578 (β) with a 6.5 Hz $^{3}J_{H,H}$ coupling constant. This signal does not change with ^{19}F decoupling (see Fig. 1) nor has it been reported in previous work. It is here tentatively assigned to a $–CH_2OH$ end-group on the basis of the chemical shift and coupling constant,

Table 4
Proton–fluorine HETCOR correlations for VDFT

δ (^{19}F)/ppm	δ (^{1}H)/ppm	Assignment of ^{19}F to ^{1}H
−91.690	2.905	A + A′–φ
−91.897	2.905	HT–φ
−92.034	Unresolved	Unresolved
−92.078	Unresolved	Unresolved
−92.191	Unresolved	Unresolved
−92.390	2.905	F–φ
−92.550	2.905, 2.753	G–φ–κ
−92.735	3.072, 2.905	B–ϕ–φ
−94.577	2.905 (2.196, 2.148, 2.083)	C′–φ–(π)
−94.659	2.905, 2.267	C–φ–o
−95.330	2.792, 1.965	H–ω–θ
−95.568	2.905, 2.358	I–φ–ν
−107.010	3.620 (2.171, 2.110, 2.083)	J–δ–(π)
−107.415	1.794	K–ρ
−113.768	3.072	E–ϕ
−114.319	2.905	L–φ
−114.423	6.360, 2.753	M–α–κ
−116.226	2.267	D–o

which are similar to those of other such groups in VDFT [10]. A second triplet is seen at 4.751 ppm (χ) with a $^{3}J_{H,H}$ coupling constant of 6.0 Hz, also assigned to a hydroxyl end group by reference to the literature [10]. Furthermore, signals between 3.650 and 3.570 ppm (Fig. 1b) show a complex pattern, but can probably be interpreted as two triplets of doublets at 3.622 ppm (δ) and 3.600 (ε) for methylene protons of hydroxylated extremities –C*H*$_2$–OH. Fig. 6a and b shows expansions for both the ^{19}F-coupled and -decoupled proton spectra of these two signals. In Fig. 6b only the doublet is seen for the δ signal, showing that the remaining coupling is to the hydroxyl proton, whereas the signal for ε remains

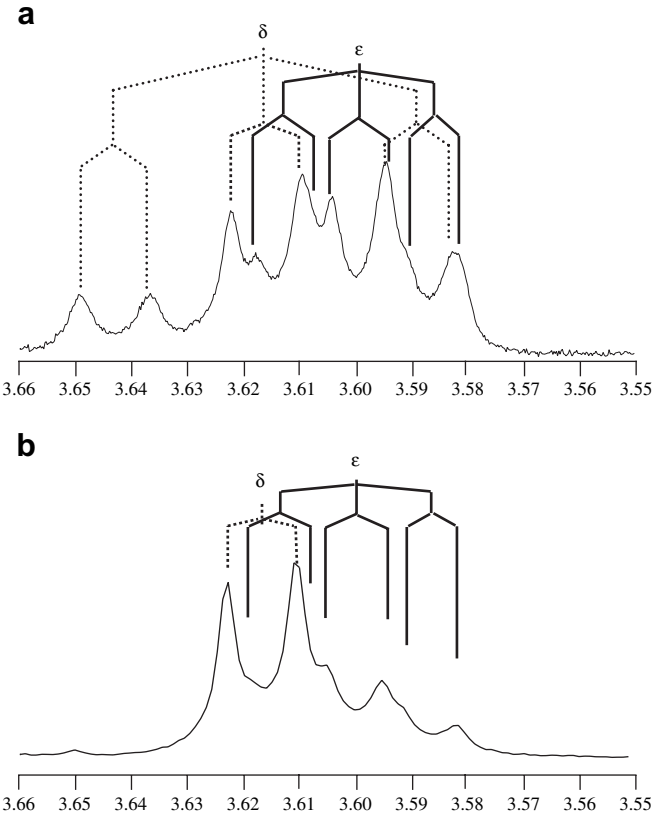

Fig. 6. Expansion of the ^{1}H spectra of VDFT in DMSO-d_6 at 22 °C between 3.66 and 3.55 ppm with ^{19}F decoupling (a) and without ^{19}F decoupling. All assignments are given in Table 1.

-CH$_2$-CF$_2$-CH$_2$-CF$_2$H
φ G κ M α

Scheme 1.

unchanged. These observations suggest that δ is for –CF$_2$C*H*$_2$OH and ε is for –CH$_2$C*H*$_2$OH. Hydroxyl structures have previously been suggested for these signals, but adjacent groups could not be determined with any great clarity [10]. Confirmation of our assignments comes from the ^{1}H COSY (Fig. 3 and Table 3), where it is clear that the signal ε couples to that labelled π at 2.138 ppm with J_{HH} ~ 6.5 Hz and to χ with ~6.0 Hz, while β couples to δ with ~6.5 Hz. Furthermore both π and δ have a $^{3}J_{F,H}$ coupling of ~14.5 Hz. The ^{1}H/^{19}F HETCOR (Fig. 5 and Table 4) shows that both π and δ correlate to the ^{19}F signal *J* at −107 ppm. This resonance is a quintet with a $^{3}J_{F,H}$ (14.5 Hz) but is a singlet when decoupled (Fig. 4a and b and Table 4). This strongly suggests that the fluorine signal at −107 ppm (*J*) derives from a short-chain species and is not associated directly with end-chain groups of the VDF polymer backbone nor is it for a branch point; the suggested structure is given in Scheme 2. The integrals of the signals confirm the structure and verify it as a reaction by-product. Perhaps of greater interest is that these alcohol groups are not part of the polymer fragment, and thus do not fulfil a major purpose of providing functionality for further chemical modification of the main polymer.

3.3. The structure of the defect units

There are several signals in the fluorine-decoupled proton spectrum (Fig. 2) at similar chemical shifts to the main-chain signal at 2.905 ppm (φ); these are at 3.072 (ϕ), 3.012 (γ), 2.997 (η), 2.963 (ι), 2.837 (ϖ) and 2.792 (ω) ppm. The fine structure of these individual signals is difficult to interpret because of signal overlap. All of them have similar linewidths (~6 Hz) to that of the main-chain signal, and therefore no $^{4}J_{H,H}$ coupling is seen. However, we do suggest that they are probably from –C*F*$_2$–C*H*$_2$–C*F*$_2$– structure types, apart from the signal ϕ, which correlates in the ^{19}F/^{1}H HETCOR spectrum with resonance E of the CF$_2$ group in the defect unit (Fig. 5). The reverse unit CH$_2$ signal (o) at 2.267 ppm correlates to the fluorine signals D and C, seen in the same spectrum; therefore, C and D must be adjacent to or part of the defect protons. The CF$_2$ reverse groups D and E couple, as shown in Fig. 7 (in spite of the lack of observable splittings in their spectra), and the proton signal ϕ couples only to E and B (Fig. 5), so ϕ is adjacent to a reverse unit. The proton signal ϕ couples to both B and A′ in the same spectrum allowing the assignment D–E–ϕ–B–φ–A′–φ. This is also verified in the ^{19}F COSY spectrum Fig. 6a and b, since E couples to B and B to A′. Furthermore, only D and C couple to the proton reverse unit signal o, verifying their positions adjacent to the reverse unit structure. As shown in Fig. 7, C couples to both F and F to A but C and A do not couple, giving A–F–C, and all couple to the main-chain proton signal φ (see Fig. 5 and Table 4) giving assignments for the fluorine and proton signals of the defect unit with their adjacent groups as in Scheme 3.

Moreover, the defect-unit signals in the expanded fluorine spectrum (Fig. 8a and b) show that the linewidths of the proton-coupled signals are ~50 Hz (E) and ~45 Hz (D). By reference to Scheme 3 and literature values [23], the signal E should be coupled by $^{4}J_{F,F}$ (~10 Hz) from signal B and $^{3}J_{F,F}$ (probably negligibly small)

HO-CH$_2$-CF$_2$-CH$_2$-CH$_2$-OH
β δ J π ε χ

Scheme 2.

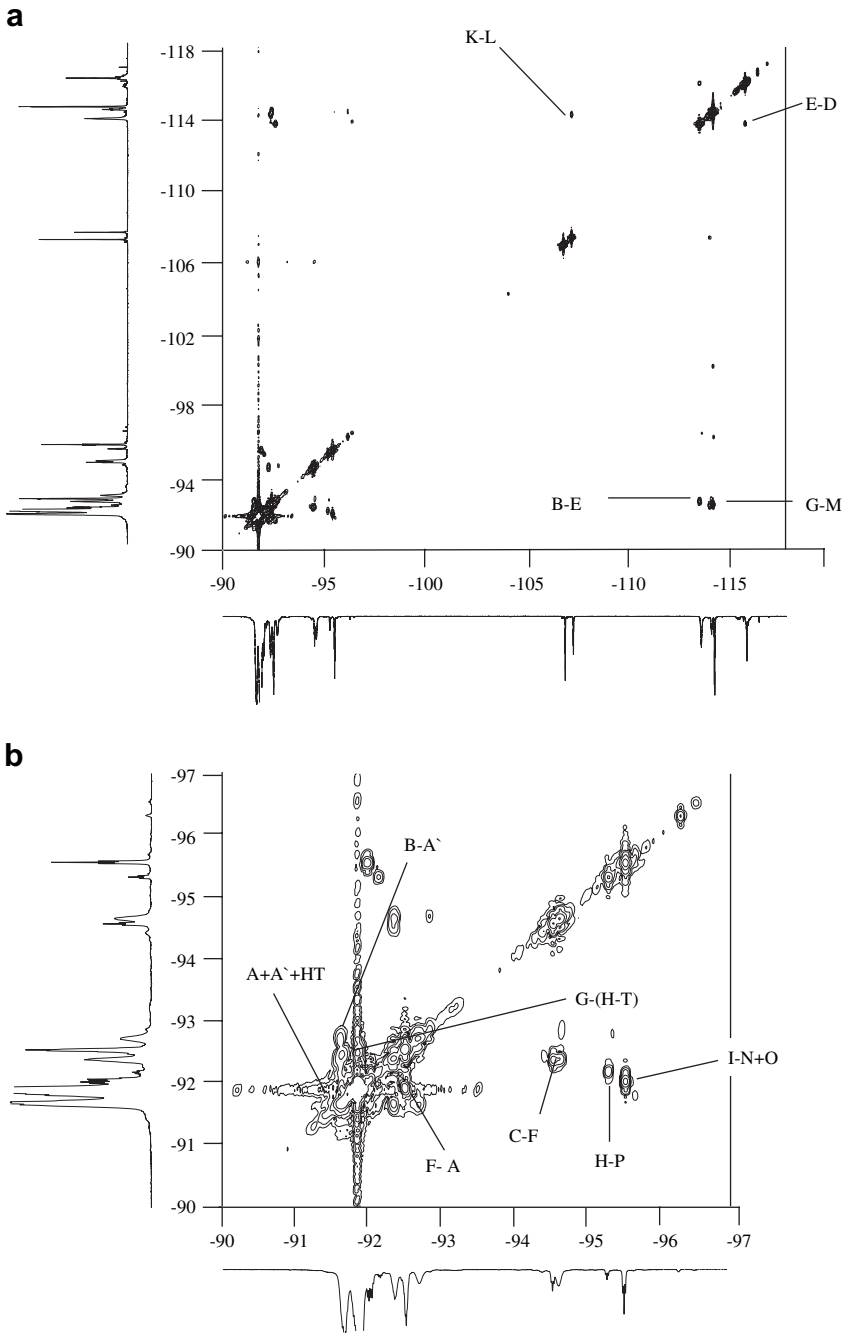

Fig. 7. ^{19}F–^{19}F COSY of the VDF telomer in DMSO-d_6 at 22 °C (a) and expansion of the region around the main-chain signals (b).

from D, but also $^3J_{F,H}$ (~16 Hz) and $^4J_{F,H}$ (~5 Hz) from ϕ and o, respectively. In the case of signal D, its largest splitting contribution would come from $^3J_{F,H}$ (~16 Hz) since literature values predict a $^3J_{F,F}$ of ~0 Hz. Both signals have widths which are reduced by one third to ~33.0 Hz (E) and ~16 Hz (D) when proton decoupled. Proton decoupling seems, therefore, to be more effective on D than E. As discussed in the Section 1, $^3J_{F,H}$ and $^4J_{F,F}$ should normally provide the strongest coupling in VDFT; the broad signal for E reflects this.

$$\text{-}CF_2\text{-}CH_2\text{-}CF_2\text{-}CH_2\text{-}CF_2\text{-}CH_2\text{-}CH_2\text{-}CF_2\text{-}CF_2\text{-}CH_2\text{-}CF_2\text{-}CH_2\text{-}CF_2\text{-}$$

A φ F φ C o o D E ϕ B φ A'

Scheme 3.

3.4. Assignments of various end groups and chain substructures

Two proton signals at 1.252 ppm (σ) and μ at 2.653 ppm are related to a minor component and not debated here.[1] The protons signal λ, giving a triplet at 2.720 ppm with $^3J_{H,H}$ (7.5 Hz) and ν, showing a triplet of triplets at 2.358 ppm with $^3J_{H,H}$ (6.5 Hz) and $^3J_{F,H}$ (16.5 Hz), correlate in the ^1H COSY (Fig. 3). The proton signal ν

[1] A proton singlet at 1.252 ppm (σ) (Figs. 1 and 2) may be assigned to the methyl groups of the *tert*-butyl alcohol (CH_3)$_3$–C–O–H produced from the radical initiator di-*tert*-butyl peroxide ((CH_3)$_3$–C–O–)$_2$, which decomposes to *t*-butyl radicals that rearrange into H_3C^+ + acetone as noted in the literature [34]. The signal μ at 2.653 ppm, which is a quartet, is a O–CH_2 group, and no further information is offered.

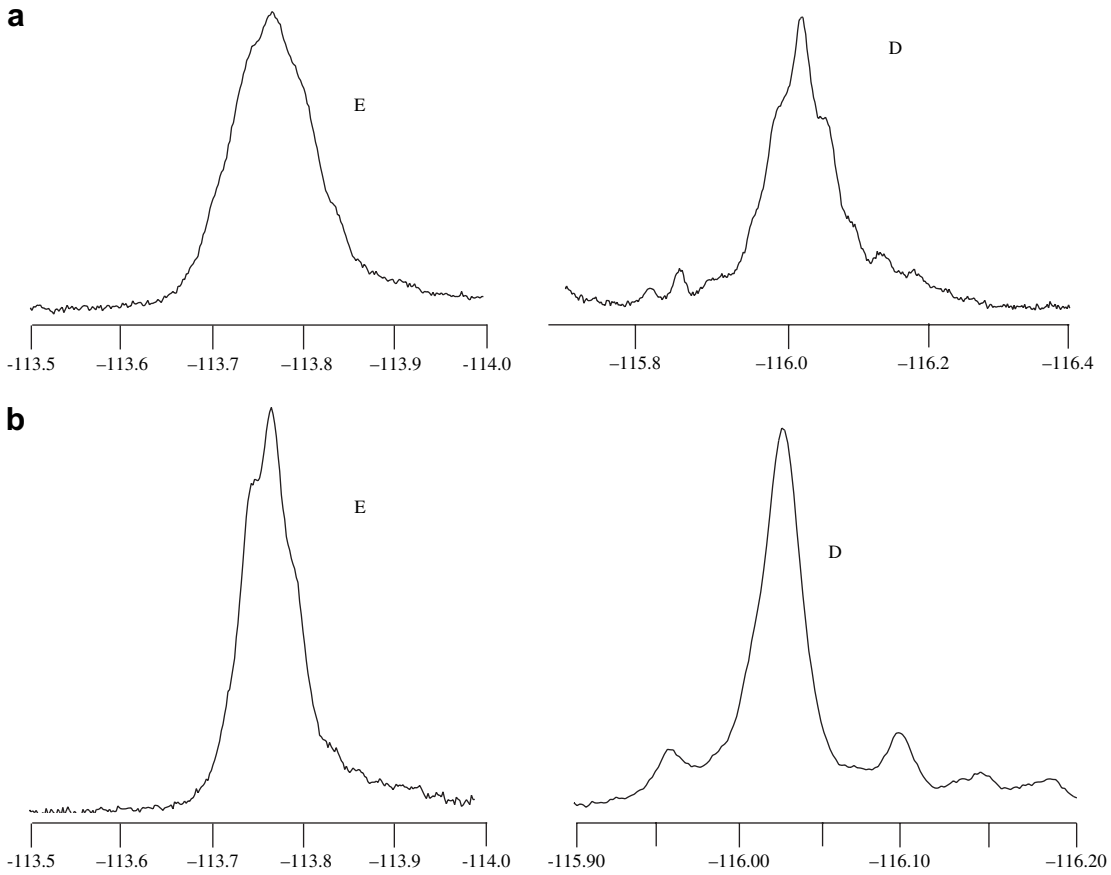

Fig. 8. Expansion of the reverse-unit signals in the ^{19}F spectrum without proton decoupling (a) and with proton decoupling (b).

and φ both correlate to the fluorine signal I at −95.568 ppm, as seen in the $^{19}F/^{1}H$ HETCOR spectrum (Fig. 5 and Table 4). As the signal λ is neither affected by ^{19}F decoupling nor is it adjacent to any fluorine group, its chemical shift would imply that an electronegative group is adjacent to it, possibly $(CH_3)_3$–C–O–, but this is speculative as the integrals do not verify this. The fragment shown in Scheme 4 is suggested.

In Fig. 1, a triplet of quartets is seen at 1.961 ppm (θ), showing $^{3}J_{H,H}$ (7.5 Hz) and $^{3}J_{F,H}$ (16.5 Hz) coupling. The proton coupling magnitude and the intensity of this signal correspond to those for the triplet at 0.967 ppm (τ), These signals also show mutual coupling in the ^{1}H COSY (Fig. 3) and the signal θ couples to a CF_2 group (H) at −95.330 ppm, as does ω seen in the $^{19}F/^{1}H$ HETCOR spectrum (Fig. 5). From the ^{19}F COSY experiment (Fig. 6), H is shown to couple to P (at −92.191 ppm), though further couplings of P are not revealed. On the basis of such assignments and integrals, these signals represent an end group, as shown in Scheme 5.

The triplet at 1.794 ppm (ρ), with a $^{3}J_{F,H}$ of 19.5 Hz (Fig. 1), is a singlet in the decoupled spectrum (Fig. 2). Furthermore, the fluorine signal K at 107.415 ppm (Fig. 4) is a quartet with the analogous $^{3}J_{F,H}$, measured as 20.0 Hz (Table 3), giving the assignment to a $–CF_2–CH_3$ end group. The $^{19}F/^{1}H$ HETCOR (Fig. 5) shows K to be coupled to ρ at 1.794 ppm but not to any other protons. Published data from unresolved spectra [10,11] suggest that this signal originates from a $CH_3–CF_2–CF_2–$ end group; indeed in the ^{19}F COSY (Fig. 7) K does couple to L at −114.319 ppm, which couples further to the main-chain proton signal φ at 2.905 ppm, giving the sub-structure depicted in Scheme 6, and all signals have commensurate relative intensities in the respective spectra. Thus K and L should involve $^{3}J_{F,F}$. However, the signal K is a singlet when proton decoupling is applied whereas L is a broad triplet with an apparent ∼10 Hz $^{3}J_{F,F}$ coupling. The coupling of L to K is questionable as the signal K, which has an 8 Hz linewidth, should also show the 10 Hz coupling seen in signal L and it does not. A possible explanation for this is that the $^{3}J_{F,F}$ coupling of K to L is smaller than 5 Hz linewidth of the signal K and the coupling of 10 Hz for L with a linewidth of 8 Hz reflects the larger $^{4}J_{F,F}$ coupling constant to the next adjacent CF_2 group shown as an asterisk in Scheme 6. This would be in agreement with the known attenuation of fluorine couplings [35,36] suggesting the end-group structure shown in Scheme 6. However, one would expect to see this $^{4}J_{F,F}$ coupling between these signals in the ^{19}F COSY spectrum, but due to poor resolution no correlation is obvious.

3.5. Short-chain oligomers showing similar ^{19}F, ^{19}F coupling

Many of the ^{19}F signals, such as H–T, F, and B, show increased resolution due to decoupling, but do not allow measurement of the magnitude of $^{3}J_{F,F}$ or $^{4}J_{F,F}$ because linewidths are 10 Hz or more. Along with signal C, these resonances are here assigned to fluorine groups adjacent to the defect units or end groups (see Section 3). The signals C, H and I also show an increase in resolution due to

X-CH_2-CH_2-CF_2-CH_2-
λ ν I φ

Scheme 4.

-CF_2-CH_2-CF_2-CH_2-CH_3
P ω H θ τ

Scheme 5.

$$\underset{*}{\text{-CF}_2\text{-}}\underset{\varphi}{\text{CH}_2\text{-}}\underset{L}{\text{CF}_2\text{-}}\underset{K}{\text{CF}_2\text{-}}\underset{\rho}{\text{CH}_3}$$

Scheme 6.

decoupling. Although the signals H and I have been discussed in previous sections, the effect of decoupling on these signals is worth a special mention here. Both the signals H and I give a $^4J_{F,F}$ of ~9.5 Hz and C is resolved into two separate signals, now labelled C′ and C (Fig. 9a and b) at −94.577 and −94.659 ppm, respectively. A $^4J_{F,F}$ of 9.5 Hz for C′ is also seen. Furthermore, new signals (N, O, and P) are observed in the region of the main-chain fluorine signal H–T at −91.897 ppm, with a $^3J_{F,F}$ of 9.5 Hz. The fluorine signals C′, H and I (Fig. 9b) are all triplets with different integral values but have very similar $^4J_{F,F}$ values of ~9.5 Hz as do N, O and P. Credible integral values for N and O are not obtainable due to insufficient resolution, but the signal P has the same integral as H and they do couple in the ^{19}F COSY spectrum, as mentioned above. The proton-coupled fluorine spectra show the signals H and I with multiplet intensities 1:2:5:8:10:12:10:8:5:2:1, which is consistent with assignment to the fluorines of systems such as –$CH_2CF_2CH_2CF_2CH_2$– (see Scheme 5), showing $^4J_{F,F}$ ~ 9.5 Hz and $^3J_{F,H}$ ~ 19 Hz.

3.6. The main-chain structures

From the ^{19}F and ^{1}H correlation spectroscopy discussed in the previous sections, it is seen that the fluorines adjacent to the defect units (A′ and F), Scheme 3, all couple to the main-chain signal (H–T), which in turn couples to G of the end group, Scheme 1 (see Fig. 7). It is also important to note here that the relative integral values of the end-group protons and fluorine signals (κ, α, G and M) in Scheme 1, are approximately double of what would be expected if these signals represented only one of the chain ends. Compare α and M representing the chain ends with both with integral values of 2 with signals o and D + E with integral values of 4. Furthermore, no other signal with corresponding integral values was found suggesting that both end groups have the same structure.

On the basis of these observations a tentative structural type (Scheme 7) for the main component in the reaction mixture can be suggested, where the end groups are the same. The end groups in Schemes 5 and 6 are in lower intensity and therefore not part of this main chain structure. The position of the (one or more) reverse units in the chain is, of course, uncertain.

3.7. Degree of polymerisation and the reverse unit

The degree of polymerisation ($\overline{DP}_{n\ cum}$) and reverse unit (RU%) content are commonly reported parameters for VDF polymers and are defined by Eqs. (1) and (2) [10]:

$$\overline{DP}_{n\ cum} = \frac{HT + A + B + C + F + G + E + D}{M} \quad (1)$$

$$RU\% = \frac{E}{HT + A + B + C + F + G + M + E + D} \quad (2)$$

The average cumulative degree of polymerisation was evaluated by integration of the fluorine signals representative of the VDF backbone, as indicated in Scheme 7 (H–T, A, B, C, D, E, F, G) and the fluorine signal M representing the end groups. Using data from the ^{1}H-decoupled ^{19}F NMR (Table 3), with Eq. (1), the degree of polymerisation is estimated to be 18 and using a molecular weight of 64 for the (–CH_2–CF_2–) unit, an average molecular weight for the VDF telomer was found to be 1200 Da. This should be compared to a degree of polymerisation of 10.7 by ^{1}H NMR without ^{19}F decoupling data and a molecular weight ~700 Da [10]. The decoupled fluorine spectrum gives a more accurate assessment of these parameters than the coupled proton spectrum and more in agreement with the size exclusion chromatography reported earlier of 2800 Da [10]. However, in the literature, proton spectra without decoupling are often used. What is also revealed in both ^{1}H (Fig. 2b) and ^{19}F (Fig. 9b) spectra with decoupling is that the main-chain signal φ and HT, respectively, have contributions from signals not associated with the polymer backbone structure or are of an unknown origin i.e. γ, ι, ϖ and ω in the proton spectrum and O, P, and N in the fluorine spectra. Further complications with respect to these measurements are seen in the proton decoupled fluorine spectrum Fig. 9b where the signal C is resolved into 2 signals C and C′, clearly originating from two different structures as seen in the

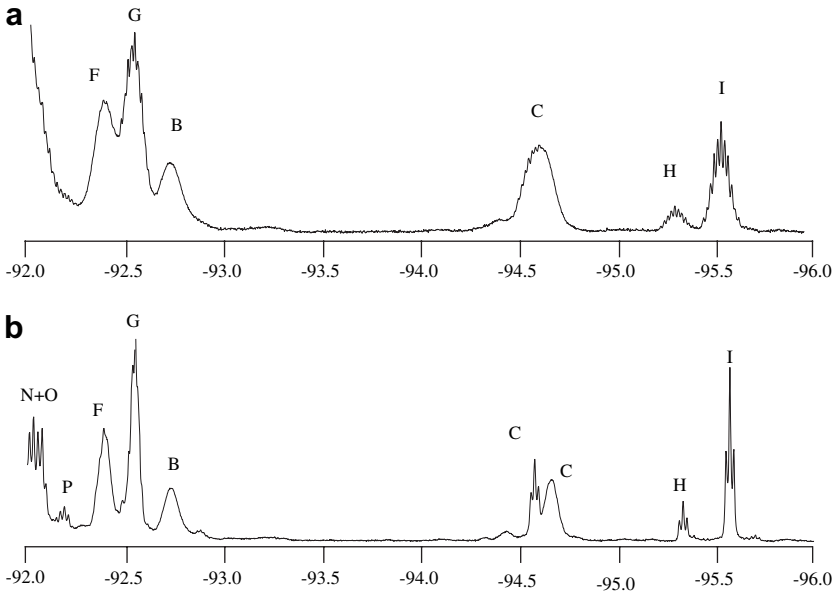

Fig. 9. Expansion of the −92 to −96 ppm region in the ^{19}F proton-coupled (a) and proton-decoupled (b) spectra of the VDF telomer in DMSO-d_6 at 22 °C, showing reverse-unit and fluorine chain-end signals.

H-CF_2-CH_2-CF_2-CH_2-[CF_2-CH_2]$_m$-CF_2-CH_2-CF_2-CH_2-CF_2-CH_2-CH_2-CF_2-CF_2-CH_2-CF_2-CH_2-CF_2-CH_2-CF_2-CH_2-CF_2-CH_2-CF_2-H

α M κ G φ H-T φ [A φ F φ C o o D E ϕ B φ A']n φ H-T φ G κ M α

Scheme 7.

correlation spectrum Fig. 5b, but often calculated as one signal in the context of degree of polymerisation and reverse unit content. All of these discrepancies originating from incorrect structural evaluation and lack of effective decoupling of spectra will lead to erroneous evaluations of reverse unit content and the degree of polymerisation.

A reverse-unit content was calculated to be 3%, using Eq. (2) with integral values from the proton-decoupled fluorine spectrum. This implies that, on average, there is one reverse unit per chain. As stated earlier, the amount of reverse units is usually large in the early stages of polymerisation, up to 50%, and decreases with increase in molecular weight [10,34]. Though earlier results gave 13–19% from both ^{1}H and ^{19}F NMR data with no decoupling, in this study, the amount of reverse units is low and comparable to other reported values for radical telomerization [37].

4. Conclusions

The decoupling of ^{19}F or ^{1}H when ^{1}H or ^{19}F NMR spectra are being acquired, respectively, results in a significant improvement in resolution, clearly seen in the ^{19}F spectra for the vinylidenefluoride telomer (VDFT) ^{19}F signals N, O, P H, I and C′, which have not been, to our knowledge, previously assigned in the literature on VDFT. Decoupling has also allowed verification of $^3J_{F,H}$ and $^4J_{F,H}$ coupling constants, which were found to be in general agreement with relevant literature values with respect to the attenuation of the coupling strength. Two structures are tentatively presented, an oligomer with a reverse unit (Scheme 7), and a small molecule (Scheme 2). As the linewidths for the higher molecular weight compound, Scheme 7, showed typical values in excess of 10 Hz, splittings arising from $^4J_{F,F}$ (~9.5 Hz) were only resolved for the small molecule. It was concluded that the proton-decoupled fluorine spectra should give more accurate values for reverse unit and end group content than coupled spectra because of the higher resolution of the signals in question. The increased resolution available from decoupling also aided the determination of new hetero- and homo-nuclear coupling constants. The fact that $^4J_{F,F}$ is generally greater than $^3J_{F,F}$ must be taken into account in the structural determination of highly fluorinated compounds. The fluorine spectrum of VDFT also shows signals of specific interest, namely J and K. We have assigned these signals to small molecular by-products and end groups, respectively, and not to branched structure as often reported in earlier publications. Signals associated with major polymer backbone structures have linewidths, which are generally equal to or greater than the magnitude of homonuclear $^3J_{F,F}$ and $^3J_{H,H}$ coupling constants, making their determination difficult. The calculation of the reverse unit content and the degree of polymerisation should be carried out on decoupled spectral data with full assignment to correctly evaluate these parameters. Although several end-group signals appear in the spectra of VDFT, the CF_2H end group was shown to provide the major method of termination of the polymer chain based on correlations and integral values and therefore this work shows that the main reaction product has reactive end groups giving the possibility of further modification.

Acknowledgments

We would like to thank Dr D.C. Apperley at the EPSRC NMR service, University of Durham for helpful discussion throughout this work.

References

[1] Ferguson RC. J Am Chem Soc 1960;82:2416.
[2] Gorlitz M, Minke R, Trautvet W, Weisgerb G. Angew Makromol Chem 1973; 29(3):137.
[3] Ferguson RC, Ovenall DW. Abstr Paper Am Chem Soc 1984;187:157.
[4] Macheteau JP, Oulyadi H, van Hemelryck B, Bourdonneau M, Davoust D. J Fluorine Chem 2000;104:149.
[5] Battiste J, Newmark RA. Prog NMR Spectr 2006;48:1.
[6] Battiste JL, Jing NY, Newmark PA. J Fluorine Chem 2004;125:1331.
[7] Boyer C, Valade D, Lacroix-Desmazes P, Ameduri B, Boutevin B. J Polym Sci Part A Polym Chem 2006;44:5763.
[8] Guiot J, Ameduri B, Boutevin B, Lannuzel T. Eur Polym J 2003;39:887.
[9] Mladenov G, Ameduri B, Kostov G, Mateva R. J Polym Sci Part A Polym Chem 2006;44:1470.
[10] Duc M, Ameduri B, Boutevin B, Kharroubi M, Sage J-M. Macromol Chem Phys 1998;199:1271.
[11] Pianca M, Barchiesi E, Esposto G, Radice S. J Fluorine Chem 1999;95:71.
[12] Russo S, Behari K, Chengji S, Pianca M, Barchiesi E, Moggi G. Polymer 1993;34: 4777.
[13] Herman, Uno T, Kubono A, Umemoto S, Kikutani T, Okui N. Polymer 1997;38: 1677.
[14] Katoh E, Ogura K, Ando I. Polym J 1994;26:1352.
[15] Kharroubi M, Manseri A, Ameduri B, Boutevin B. J Fluorine Chem 2000;103: 145.
[16] Manseri A, Ameduri B, Boutevin B, Chambers RD, Caporiccio G, Wright AP. J Fluorine Chem 1995;74:59.
[17] Duc M, Ameduri B, David G, Boutevin B. J Fluorine Chem 2007;128:144–9.
[18] Ameduri B, Boutevin B, Kostov GK, Petrova P. Des Monomers Polym 1999;2: 267.
[19] Raulet R, Grandclaude D, Humbert F, Canet D. J Magn Reson 1997;124:259.
[20] Jones BG, Branch SK, Threadgill MD, Wilman DEV. J Fluorine Chem 1995;74: 221.
[21] Bailey WI, Kotz AL, McDaniel PL, Parees DM, Schweighardt FK, Yue HJ, et al. Anal Chem 1993;65:752.
[22] Bruch MD, Bovey FA, Cais RE. Macromolecules 1984;17:2547–51.
[23] Cais RE, Kometani JM. Macromolecules 1985;18:1354–7.
[24] Wormald P, Apperley DC, Beaume F, Harris RK. Polymer 2003;44:643.
[25] Yu HJM, Ni HJC. J Microwave Radiofreq Spectrosc 1984;1:372.
[26] Muracheva YM, Shashkov AS, Dontsov AA. Polym Sci USSR 1981;23:711.
[27] Sauguet L, Ameduri B, Boutevin B. J Polym Sci Part A Polym Chem 2007;45: 1814.
[28] Souzy R, Ameduri B. Prog Polym Sci 2005;30:644.
[29] Wormald P, Ameduri B, Harris RK, Hazendonk P. Solid State NMR 2006;30:114.
[30] Hazendonk P, Harris RK, Ando S, Avalle P. J Magn Reson 2003;162:206.
[31] Ando S, Harris RK, Hazendonk P, Wormald P. Macromol Rapid Commun 2005; 26:345.
[32] Ando S, Harris RK, Reinsberg SA. Magn Reson Chem 2002;40:97.
[33] Diehl P, Harris RK, Jones RG. Prog NMR Spectrosc 1967;3:1.
[34] Kostov G, Ameduri B, Boutevin B. Macromol Chem Phys 2002;203:1763.
[35] Berger S, Braun S, Kalinowski H-O. NMR spectroscopy of the non-metallic elements. New York: Wiley; 1997.
[36] Schwarz R, Seelig J, Kunnecke B. Magn Reson Chem 2004;42:512–7.
[37] Ameduri B, Ladaviere C, Delolme F, Boutevin B. Macromolecules 2004;37: 7602–9.